Neuropsychologia 87 (2016) 144–156

Contents lists available at ScienceDirect

Neuropsychologia

journal homepage: www.elsevier.com/locate/neuropsychologia

The role of vision in the neural representation of unique entities

Xiaoying Wang [a], Marius V. Peelen [b], Zaizhu Han [a], Alfonso Caramazza [b,c], Yanchao Bi [a,*]

[a] National Key Laboratory of Cognitive Neuroscience and Learning and IDG/McGovern Institute for Brain Research, Beijing Normal University, Beijing 100875, China
[b] Center for Mind/Brain Sciences, University of Trento, 38068 Rovereto, Italy
[c] Department of Psychology, Harvard University, Cambridge, MA 02138, United States

ARTICLE INFO

Article history:
Received 18 January 2016
Received in revised form
2 May 2016
Accepted 8 May 2016
Available online 10 May 2016

Keywords:
Congenitally blind
Visual experience
Precuneus
Anterior temporal lobe
Unique entity

ABSTRACT

Famous places and famous people are different from their common counterparts in that we have unique knowledge about individual items, including specific knowledge about their visual appearance and other sensory properties. Previous studies have shown that the processing of unique entities selectively activates a network of brain regions that includes the bilateral anterior temporal lobes (ATL), posterior cingulate cortex and adjacent medial precuneus (PCC/medPrec), medial prefrontal cortex (medPFC), and temporal-parietal junction (TPJ). The degree to which these regions represent visual properties associated with famous people/places is unknown. Here we compared fMRI responses in congenitally and sighted individuals to test whether visual experience contributes to the development of unique-entity responses in these regions. Names of unique entities (famous places, famous people) and generic items (daily scenes such as "bridge", face parts) were presented aurally to 13 congenitally blind and 16 sighted participants. Sighted participants additionally viewed corresponding photographs. We found that bilateral PCC/medPrec, medPFC, left TPJ, left ATL and right superior frontal gyrus were more strongly activated by pictures of unique entities compared to generic items. Importantly, all regions showed similar selectivity for unique entities in both groups when only names were presented. Furthermore, resting-state functional connectivity analysis revealed that these regions were tightly interconnected in both groups. Together, these results provide evidence for a visually-independent brain network underlying unique entity processing.

1. Introduction

Unique entities, such as an individual person or place, are entities that are processed at the most specific conceptual level and thus each of them is in a class with no other members (Grabowski et al., 2001). The study of the neural mechanisms underlying the processing of unique entities has gained important insights from the comparison between famous places or people and their common counterparts (e.g., the Leaning Tower of Pisa vs. a regular tower; J. F. Kennedy vs. an unknown man), as these famous entities are the set of unique entities commonly known across individuals. Neuropsychological and neuroimaging studies have shown that the processing of famous entities, relative to non-famous ones, is more strongly associated with a distributed network of brain regions (Damasio et al., 1996; Fairhall and Caramazza, 2013; Fairhall et al., 2014; Gesierich et al., 2012; Gorno-Tempini and Price, 2001; Gorno-Tempini et al., 1998; Grabowski et al., 2001; Nakamura et al., 2000; Ross and Olson, 2012; Tranel, 2006), which include bilateral anterior temporal lobes (ATL), the posterior cingulate cortex and adjacent medial precuneus (PCC/medPrec), medial prefrontal cortex (medPFC), and temporal-parietal junction (TPJ). The specific role of these regions in the processing of unique entities is not fully understood.

Several properties that tend to distinguish famous people and places from their common counterparts could underlie the brain activations previously observed (e.g., Ross and Olson, 2012): they are associated with specific semantic knowledge (e.g., the Leaning Tower of Pisa is the tilting tower in Italy where the scientist Galileo performed his gravity experiment); they are denoted by a proper name ("the Leaning Tower of Pisa"); and they are often associated with episodic memories (e.g., the episode when you saw a documentary about the tower). Importantly, compared to generic object concepts (e.g., a tower), whose mental representation tends to be prototypical or fuzzy, an individual entity is associated with richer and more specific perceptual knowledge. Some (e.g., the Leaning Tower of Pisa) are associated with fleshed out visual characteristics, with specific details of shape, color, size, and/or

* Corresponding author.
E-mail address: ybi@bnu.edu.cn (Y. Bi).

http://dx.doi.org/10.1016/j.neuropsychologia.2016.05.007

configuration; others may depend more on auditory properties, such as compositions or songs (the opening bars of Beethoven's *5th symphony*; Bruce Springsteen's *Born in the USA*). There are also individual concepts whose physical properties can only be imagined, such as characters and places in novels. Is specific sensory experience the basis for the differences of brain activations between generic concepts and famous entities presented above? One direct way to study this question is to examine whether the absence of a particular type of sensory experience modulates the relevant brain regions' responses to unique entities, for instance, in the cases of congenital blindness. The logic is that if a region processes visually-determined properties of unique entities, then the preference for unique entities is absent in the congenitally blind population; if, on the other hand, the unique-entity preference reflects properties of unique entities that are established independently of vision, such as the nonvisual variables sketched above, similar unique entity effects in sighted and blind groups are predicted.

In the present study, we tested the extent to which the brain regions that have been implicated in the processing of unique entities depend on visual experience with unique entities. Though the brain regions showing a preference for unique entities were found to be multimodal in previous literature (Binder and Desai, 2011; Ghazanfar and Schroeder, 2006; Lambon Ralph, 2014; Visser et al., 2010), visual input might play a critical role in differentiating unique entities from their common counterparts in these regions. The possibility that stronger activity to unique entities might reflect the retrieval of visual knowledge is particularly relevant for regions in temporal cortex: the bilateral ATLs are traditionally considered to be the end point of the ventral visual pathway (Gross, 1994; Gross et al., 1969; Kravitz et al., 2013). Studies on macaques and humans have found that the right ATL differentiates between individual faces (Freiwald and Tsao, 2010; Kriegeskorte et al., 2007; see Anzellotti and Caramazza, 2014 for a review), suggesting that it represents high-level visual information specific to individual entities. The unique entity effects in PCC/medPrec, medPFC, TPJ and hippocampal structures may also be modulated by visual experience. For example, the anterior parts of the bilateral precuneus are strongly activated by episodic retrieval of imageable word pairs compared to non-imageable ones (Fletcher et al., 1995) and considered to be an important neural substrate of visual imagery during episodic retrieval (Buckner et al., 1995; Fletcher et al., 1996; Halsband et al., 1998; but see Krause et al. (1999) for an opposite view). The bilateral ventral IPLs have been found to be involved in the interaction between visual attention and episodic retrieval, allowing for successful memory retrieval (Guerin et al., 2012).

To examine the role of vision in the representation of unique entities we compared brain activity between congenitally blind and sighted individuals. Both groups listened to names of unique entities (famous places, famous people) and generic items (daily scenes such as “bridge”, face parts such as “mouth”). Sighted participants additionally performed a visual experiment viewing photographs of these items such that visual properties of these entities were directly available for the participants. The generic items shown in the pictures were not personally familiar to the participants. Regions showing a “selective” response to unique entities only in the sighted group likely represent visually-determined properties of unique entities, whereas regions showing similar unique entity effects in both sighted and blind groups more likely reflect properties of unique entities that are established independently of vision. The way in which the relevant regions are intrinsically interconnected was also compared between groups using resting-state fMRI measures to further examine whether the absence of visual experience changes the information communication patterns. Note that face parts, rather than whole faces, were used as the generic baseline for famous people because of the limitation of finding stimuli for the auditory experiments. This is not an ideal baseline because it differs from famous people not only in terms of uniqueness but also in visual and semantic aspects. We thus performed both analyses using the places and people stimuli together and also separate analyses using only the places conditions (famous places and generic daily scenes) for whole brain contrasts.

2. Materials and methods

2.1. Participants

Thirteen congenitally blind (4 females) and 16 sighted controls (7 females) participated in the main fMRI experiment. The blind and the sighted groups were matched on handedness (all right-handed), age (blind: mean $\pm$ SD$=38\pm12$, range$=18-58$; sighted: mean$\pm$SD$=43\pm11$, range $=26-59$; $t_{(27)}<1$) and years of education (blind: mean $\pm$SD$=11\pm3$, range$=0-12$; sighted: mean$\pm$SD$=12\pm2$, range$=9-15$; $t_{(27)}<1$). Resting-state fMRI scanning was performed on 14 congenitally blind (7 females; mean age$=45$, range$=26$–60) and 34 right-handed sighted participants (20 females; age: mean $\pm$SD$=22.5\pm1.3$, range$=20$–26) in separate studies (Peelen et al., 2013; Wei et al., 2012). Nine of these 14 blind subjects also participated in the main fMRI experiment. All blind participants reported that they had been blind since birth. None of the participants remembered to have ever been able to visually recognize shapes. Because medical records of onset of blindness were not available for most participants, it is not possible to rule out that some may have had vision very early in life. All blind participants were examined by an ophthalmologist to confirm their blindness and to establish the causes if possible. See Table 1 for detailed information about the congenitally blind participants.

All participants were native Mandarin Chinese speakers. None had any history of psychiatric or neurological disorders or suffered from head injury. All participants provided informed consent and received monetary compensation for their participation. The study was approved by the institutional review board of the Beijing Normal University (BNU) Imaging Center for Brain Research.

2.2. Stimuli

The experiments consisted of pictures or names of objects belonging to 18 categories. The 4 conditions that were relevant for the present paper were the two categories of famous entities (famous places, famous people) and the two categories of corresponding generic entities (daily scenes, face parts), each containing 18 items (see Appendix for a complete list of stimuli). The other conditions were included to study object category representations in the ventral stream, and are reported separately (Wang et al., 2015).

In the visual experiment, stimuli were gray-scale photographs (400×400 pixels, $10.55^\circ\times10.55^\circ$ of visual angle); in the auditory experiments they were entity names that were digitally recorded (22,050 Hz, 16 Bit), spoken by a female native Mandarin speaker. Stimulus presentation was controlled by E-prime (Schneider et al., 2002). The photographs of the daily scenes and face parts were images that the sighted participants were not personally familiar with (see Fig. 1(A) for example).

2.3. Design and task

In the main experiment, a size judgment task was adopted using a block design (He et al., 2013; Mahon et al., 2009; Peelen

Table 1
Background information of congenitally blind participants.

Subject	Age and gender	Years of education	Cause of blindness	Light Perception	Reported age at blindness onset	Experiments participated
1	21, M	12	congenital microphthalmia	none	0	T
2	18, M	12	congenital glaucoma and cataracts	none	0	T
3	23, M	0	congenital anophthalmos	none	0	T
4	30, M	12	congenital microphthalmia and microcornea	none	0	T
5	38, F	12	congenital glaucoma	none	0	Both
6	45, M	12	congenital microphthalmia;cataracts; leukoma	none	0	Both
7	44, F	9	congenital glaucoma	none	0	Both
8	46, F	12	cataracts; congenital eyeball dysplasia	faint	0	Both
9	53, M	12	congenital eyeball dysplasia	none	0	Both
10	36, M	12	congenital leukoma	faint	0	Both
11	36, F	12	congenital optic nerve atrophy	faint	0	Both
12	58, M	9	congenital glaucoma and leukoma	none	0	Both
13	41, M	12	congenital glaucoma	none	0	Both
14	28, F	15	congenital microphthalmia; microcornea; leukoma	faint	0	R
15	37, F	12	–	faint	0	R
16	60, M	12	–	faint	0	R
17	46, M	12	–	faint	0	R
18	54, F	9	–	faint	0	R

Note: T: task-fMRI; R: resting-state fMRI; -, no professional medical establishment of cause of blindness.

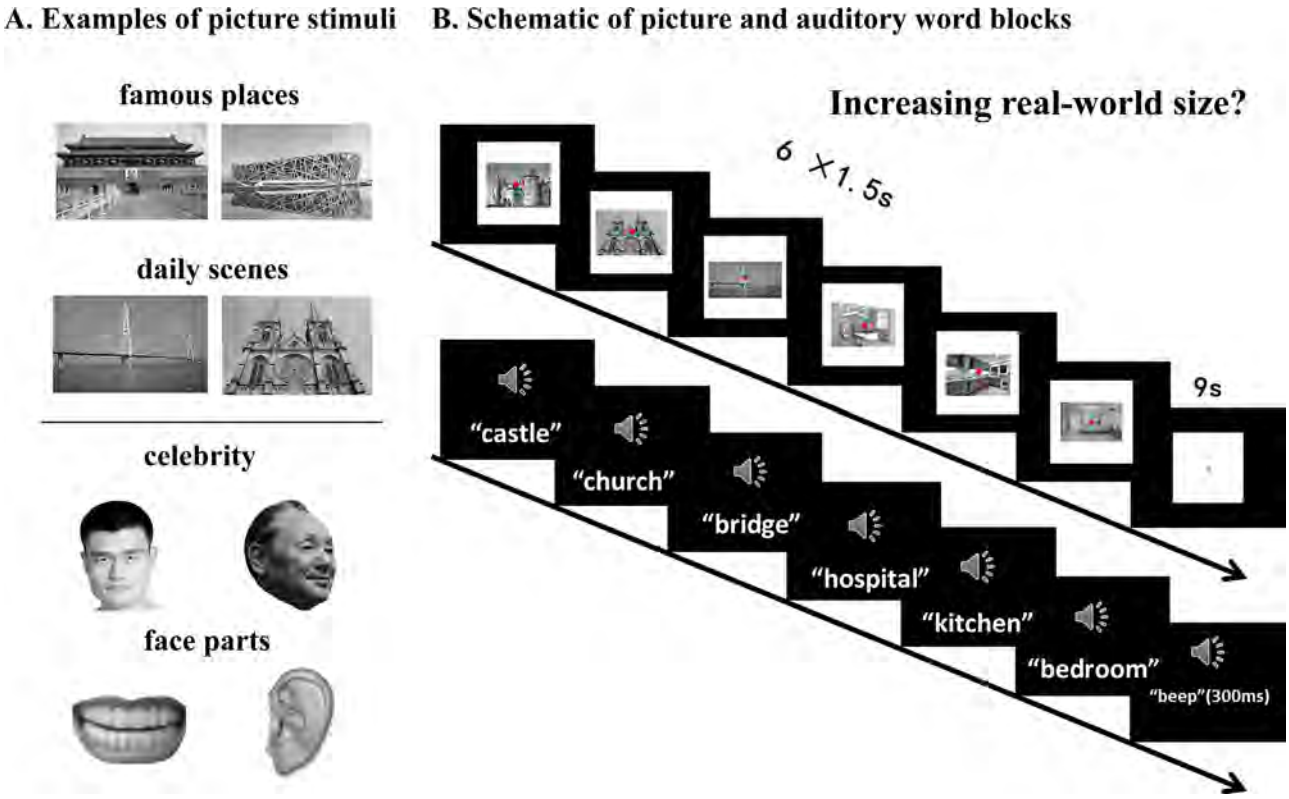

Fig. 1. Examples of picture stimuli (A) and schematics of picture and auditory word blocks (B).

et al., 2013; Wang et al., 2015) in order to encourage participants to retrieve object information. The auditory and the visual version of the experiment had the same structure. Each experiment consisted of 12 runs, with each run lasting 348 s. Each run started and ended with a 12 s fixation (visual experiment) or silence (auditory experiment) block and in between were eighteen 9 s stimulus blocks (each from one category) with an inter-block interval of 9 s For each stimulus block, six 1.5 s items from the same category were presented sequentially. Each item was presented for 4 times in total across the experiment. For each category, in half of the blocks items were arranged in an order of increasing real-world size, while for the remaining blocks the items were in random order. The order of the 12 runs and the 18 blocks within each run was pseudo-randomized across participants. See Fig. 1 for an overview of the experimental paradigm.

2.3.1. Auditory experiment

All participants were asked to keep their eyes closed throughout the experiment and to listen carefully to groups of six spoken words presented binaurally through a headphone. Participants were instructed to think about each item and press a button with the right index finger if the items were presented in an ascending

order in terms of real-world size and press the other button with the right middle finger otherwise. Responses were made after the onset of a response cue (300 ms auditory tone) immediately following the last item of the block (Fig. 1(B)).

2.3.2. Visual experiment

Sighted participants viewed the stimuli through a mirror attached to the head coil. The stimuli were gray-scale photographs presented at the center of the screen. Participants performed a size judgment task that was similar to the auditory experiment. For the famous people category, participants were asked to judge whether the items were presented in an ascending order of height. Responses were made when the fixation dot at the center of the screen turned from red to green right after the offset of the last item of the block (Fig. 1(B)).

2.4. Image acquisition

All functional and structural MRI data were collected using a 3T Siemens Trio Tim Scanner at the BNU MRI center. For the auditory and visual fMRI experiments, high-resolution anatomical three-dimensional magnetization-prepared rapid gradient echo (MPRAGE) images were collected in the sagittal plane (144 slices, TR =2530 ms, TE =3.39 ms, Flip Angle =7°, Matrix Size=256 × 256, Voxel Size =1.33 × 1 × 1.33 mm^3). BOLD activity was measured with an EPI sequence that covered the whole cerebral cortex and most of the cerebellum (33 axial slices, TR=2000 ms, TE =30 ms, Flip Angle =90°, Matrix Size=64 × 64, Voxel Size=3 × 3 × 3.5 mm^3 with gap of 0.7 mm).

Fourteen congenitally blind and 34 sighted participants underwent a resting-state scan in separate studies (see *Participants*). Participants were instructed to close their eyes and to not fall asleep. The resting-state scan lasted 6 min and 40 s for the congenitally blind group and 8 min for the sighted group. For the 14 blind participants, a T1-weighted MPRAGE structural image with the same scanning parameters as reported above, and 200 volumes of resting-state functional images using echoplanar imaging sequence (32 axial slices, TR=2000 ms, TE=33 ms, Flip Angle=73°, Matrix Size=64 × 64, FOV=200 × 200 mm^2, slice thickness=4 mm, interslice gap=0.8 mm) were acquired. For the 34 sighted participants, a T1-weighted structural MPRAGE image in sagittal plane (128 slices; TR=2530 ms, TE=3.39 ms, Flip Angle=7°, FOV=256 × 256 mm^2, slice thickness=1.33 mm, voxel size=1.3 × 1 × 1.3 mm^3) and 240 volumes of resting-state functional images using echoplanar imaging sequence (33 axial slices, TR=2000 ms, TE=30 ms, Flip Angle=90°, Matrix Size=64 × 64, FOV=200 × 200 mm^2, slice thickness=3 mm, interslice gap=0.6 mm).

2.5. Data preprocessing

Auditory and visual experiment data were preprocessed using Statistical Parametric Mapping software (SPM8; http://www.fil.ion.ucl.ac.uk/spm/) and the advanced edition of DPARSF V2.1 (Chao-Gan and Yu-Feng, 2010). The first six volumes (12 s) of each functional run were discarded for signal equilibrium. Functional data were motion-corrected, low-frequency drifts removed with a temporal high-pass filter (cut-off: 0.008 Hz), and normalized into the Montreal Neurological Institute (MNI) space using unified segmentation. The functional images were then resampled to 3 mm isotropic voxels. Functional data were spatially smoothed using a 6 mm full width at half maximum (FWHM) Gaussian kernel.

Resting-state data were preprocessed and analyzed using SPM 8, DPARSF V2.1 and Resting-State fMRI Data Analysis Toolkit V1.5 (Song et al., 2011). Functional data were resampled to 3 × 3 × 3 mm^3 voxels. The first 6 min 40 s of the sighted group's resting-state data were analyzed so that the two subject groups have matching length of resting-state time-series. The first 10 volumes of the functional images were discarded. Preprocessing of the functional data included slice timing correction, head motion correction, spatial normalization to the MNI space using unified segmentation, spatial smoothing with 6 mm FWHM Gaussian kernel, linear trend removal and band-pass filtering (0.01–0.1 Hz). Six head motion parameters, white matter and cerebrospinal fluid signals were regressed out as nuisance covariates. White matter and cerebrospinal fluid signals were calculated as the mean signals in SPM's white matter mask (white. nii) thresholded at 90% and cerebrospinal fluid mask (csf. nii) thresholded at 70%, respectively (Chao-Gan and Yu-Feng, 2010). Two participants with excessive head motion (> 2 mm maximum translation or 2°rotation) were excluded from subsequent analysis.

2.6. Data analysis

Auditory and visual experiment data were analyzed using the general linear model (GLM) in SPM8. For both experiments, a canonical hemodynamic response function (HRF) was convolved with 18 hemodynamic-response predictors corresponding to the 18 category blocks (duration=9 s) along with one regressor of no interest for the button presses (duration =0 s) for each block and six regressors of no interest corresponding to the six head motion parameters in each run. For each participant, runs in which the participant's head motion was greater than 3 mm or 3° were deleted and the remaining runs (all more than 8 runs) were entered into the analysis. Beta weights were determined for the 18 regressors for the 18 categories in each voxel for each participant while further analyses described below were based on the 4 categories we were interested in. Note that all statistical analyses below were conducted within a gray matter mask which was defined as voxels with a probability of gray matter higher than 0.4 in the SPM5 template and within the cerebral regions (#1 - #90) in the Automated Anatomical Labeling template (Tzourio-Mazoyer et al., 2002).

We first carried out a whole-brain conjunction analysis (Nichols et al., 2005) to identify regions showing significant unique entity effects in the visual experiment: random-effect GLM analyses were conducted for famous places > daily scenes and famous people > face parts, each separately meeting the significance threshold of AlphaSim corrected $p < 0.05$ (single voxel $p < 0.01$, cluster size ≥ 891 mm^3) within the gray matter mask. Overlapping regions were considered unique entity specific regions.

Given our primary interest in understanding whether regions showing unique entity preference in the sighted group are visually determined, we carried out the in-depth analyses to compare the activation preference in auditory experiments of sighted and blind groups in these regions. Specifically, for each ROI, beta values were extracted and averaged across voxels for each condition in the sighted auditory and blind auditory experiments. Two-way mixed-design ANOVAs were carried out for the place category and people category separately, with visual experience as between-group factor (blind vs. sighted) and uniqueness as within-group factor (famous vs. non-famous).

To further examine unique entity effects in the auditory experiments, we also conducted whole-brain conjunction analyses to identify unique entity specific regions in the sighted auditory and blind auditory experiments. For each auditory experiment, random-effect GLM analyses were conducted for famous places > daily scenes and famous people > face parts, each separately meeting the significance threshold of AlphaSim corrected $p < 0.05$ (single voxel $p < 0.01$, cluster size ≥ 891 mm^3) within the whole-

cerebrum gray matter mask. Overlapping regions were considered unique entity specific regions. To locate unique entity specific regions independent of visual input and visual experience, a further conjunction was conducted by overlapping regions showing significant unique entity effects across all three experiments.

In addition to the above analyses, whole-brain group-by-uniqueness ANOVAs were also conducted to more comprehensively explore the potential differences between blind and sighted groups in terms of unique entity effects. Specifically, two-way mixed effect whole-brain ANOVAs were conducted for place and people categories respectively, with visual experience as between-group factor (sighted vs. blind) and uniqueness as within-group factor (famous vs. non-famous). Significance threshold for the main effects and the interaction effect of each ANOVA was set as AlphaSim corrected $p < 0.05$ (single voxel $p < 0.01$, cluster size ≥ 891 mm^3) within the gray matter mask.

ROI-based resting-state functional connectivity analysis was then performed. The seed ROIs were defined as unique entity preferring regions identified in the sighted visual experiment. For each participant, the mean time series of the seed ROIs were correlated with each other to construct a brain network. The resulting correlation values were Fisher transformed. One-sample *t*-tests were conducted to identify significant edges connecting each pair of ROIs (Bonferroni corrected, alpha < 0.05). The strength of each edge was compared between the sighted and congenitally blind groups by using two-sample *t*-tests (Bonferroni corrected, alpha < 0.05). We further examined the strengths of RSFCs between the seed ROIs and a control site to rule out the possibility that the potential network being observed was simply driven by confounding noise. The control site was defined as a 6 mm-radius sphere centered at the MNI coordinates of $-45, -81, 20$ in the left lateral occipitotemporal cortex, a region that was found to represent object shape in a subject cohort similar to the current study (Peelen et al., 2014).

Finally, as explained in the Introduction, the famous vs. non-famous contrast of the people condition was not ideal, as face parts differed from famous people in both uniqueness and other aspects such as visual properties and semantic information. In addition, there was a slight task difference between the famous people and the face part conditions (Section 2.3, Design and Tasks), which further complicates the interpretation of these results. We thus performed a separate validation analysis where the contrast between famous places and daily scenes was taken as the main contrast to investigate the unique entity-specific effects in the whole brain analyses, on the basis of which ROI and whole-brain conjunction analyses were further carried out. Detailed information of the validation analyses is presented in the Supplementary Materials.

All results in this paper are shown in the MNI space and projected onto the MNI brain surface using the BrainNet viewer (http://www.nitrc.org/projects/bnv/) (Xia et al., 2013).

3. Results

3.1. Behavioral results

In the size judgment tasks, participants compared the real-world size of the six items in each block, indicating whether items were presented in an order of increasing real-world size. Note that it is difficult to assess the accuracy as some items have comparable sizes and subjects' judgments varied to some extent. We nonetheless checked whether the different conditions were associated with systematically different response patterns to rule out potential peripheral differences such as differences in the number of button presses: The proportion of the "increasing order" responses was on average 43% for the sighted visual experiment (57% for famous places, 47% for daily scenes, 37% for famous people, and 32% for face parts), 41% for the sighted auditory experiment (52% for famous places, 44% for daily scenes, 30% for famous people, and 36% for face parts) and 41% for the blind auditory experiment (52% for famous places, 47% for daily scenes, 32% for famous people, and 33% for face parts). There were no significant differences between famous places and daily scenes or between famous people and face parts in any experiment (all $p_s > 0.05$). The visual and auditory experiments in sighted group were also comparable across all conditions ($t_{s(15)} < 1.3$, $p_s > 0.05$), as were the two auditory experiments of sighted and blind groups ($t_{s(27)} < 1$, $p_s > 0.05$).

3.2. Unique entity effects in sighted visual experiment

A whole-brain random-effects contrast between famous places and daily scenes in the sighted visual experiment activated areas of bilateral PCC/medPrec, bilateral medPFC including superior and middle frontal cortex, anterior cingulate cortex and rectus gyrus, and small clusters in left putamen, left ATL including the anterior part of middle and inferior temporal gyrus, left TPJ including the angular gyrus and posterior parts of the middle and superior temporal gyrus, and right superior frontal gyrus (SFG). See Table 2 and Fig. 2(A) for detailed information including peak coordinates, t values, and cluster sizes.

A whole-brain random-effects contrast between famous people and face parts in the sighted visual experiment revealed a set of regions that partly overlapped the famous place contrast (Table 2 and Fig. 2(A)): bilateral medPFC including the superior and middle frontal cortices, anterior cingulate cortex and rectus gyrus, bilateral PCC/medPrec and adjacent posterior cingulate cortex, lingual gyrus and calcarine, bilateral TPJs including the angular gyrus, inferior posterior lobule, supramarginal gyrus and posterior superior and middle temporal gyrus, bilateral ATLs, bilateral hippocampus and parahippocampal gyrus (HG/PHG), left middle frontal gyrus and right inferior frontal gyrus.

A conjunction analysis (Nichols et al., 2005) revealed brain regions underlying the selective processing of both famous places and famous people, which included the bilateral PCC/medPrec, medPFC, left ATL, left TPJ and right SFG (Table 2 and green patches in Fig. 2(A)). These results are consistent with previous studies investigating the representation of unique entities (Gesierich et al., 2012; Gorno-Tempini et al., 1998; Grabowski et al., 2001; Ross and Olson, 2012).

3.3. Unique entity effects in the auditory experiments: ROI analysis

The regions identified by the whole-brain conjunction analysis of the sighted visual experiment (green patches in Fig. 2(A)) were defined as regions of interest (ROIs) to test for unique entity effects in the auditory experiments of the blind and sighted groups.

For each ROI, we carried out two-way mixed design ANOVAs, separately for the place and person categories, with group as a between-subject factor (blind vs. sighted) and uniqueness (famous, non-famous) as a within-subject factor. Of interest was whether there were unique entity effects in the place or the person category in the auditory experiments (main effect of uniqueness) and whether these effects were modulated by visual experience (group by uniqueness interaction).

All five ROIs showed significant main effects of uniqueness, for both the place and the person categories (Table 3). None of the ROIs showed an interaction between group and uniqueness (Table 3). These results indicate that the unique entity effects in the bilateral PCC/medPrec, bilateral medPFC, left TPJ, left ATL and right SFG generalized to the auditory modality, for both place and

Table 2
Unique entity-specific effects in the sighted visual experiment.

	Brain regions	BA	Peak MNI coordinates x	y	z	Peak t value	Cl. Size (voxels)
famous people versus face parts	Bilateral PCC/medPrecuneus	7/17/18/19/23/29/30/31	−3	−48	30	15.21	1059
	Right ATL	20/21/38	60	−3	−24	10.84	349
	Left ATL	20/21/22/38/47	−54	−6	−24	9.41	617
	Bilateral medPFC	6/8/9/10/11/25/32	−6	54	−9	9.21	1909
	Left TPJ	7/19/39/40	−54	−69	30	8.50	280
	Right HG/PHG	28/34/35	21	−9	−15	8.45	98
	Left MFG	10/11	−33	48	−12	7.65	44
	Right TPJ	7/21/22/39/40	54	−66	33	7.13	363
	Left HG/PHG	28/34/35	−15	−9	−18	6.03	60
	Right orbital IFG	11/47	39	39	−9	5.48	93
famous places versus daily scenes	Bilateral PCC/ medPrec	7/23/29/30/31	−3	−60	30	6.53	810
	Bilateral medPFC	6/8/9/10/11/24/25/32	−9	63	12	6.49	1359
	Left TPJ	19/39/40	−48	−66	27	4.68	93
	Left Putamen	–	−21	3	−6	4.45	47
	Left ATL	21	−63	−6	−15	4.39	61
	Right SFG/MFG	8/9	18	42	39	4.26	102
Overlapping voxels	Bilateral medPFC	8/9/10/11/25/32					680
	Bilateral PCC/medPrec	7/23/29/30/31					585
	Right SFG/MFG	8/9					91
	Left TPJ	19/39/40					74
	Left ATL	21					59

Notes: HG: hippocampus gyrus; PHG: parahippocampal gyrus; SFG: superior frontal gyrus; MFG: middle frontal gyrus; IFG: inferior frontal gyrus.

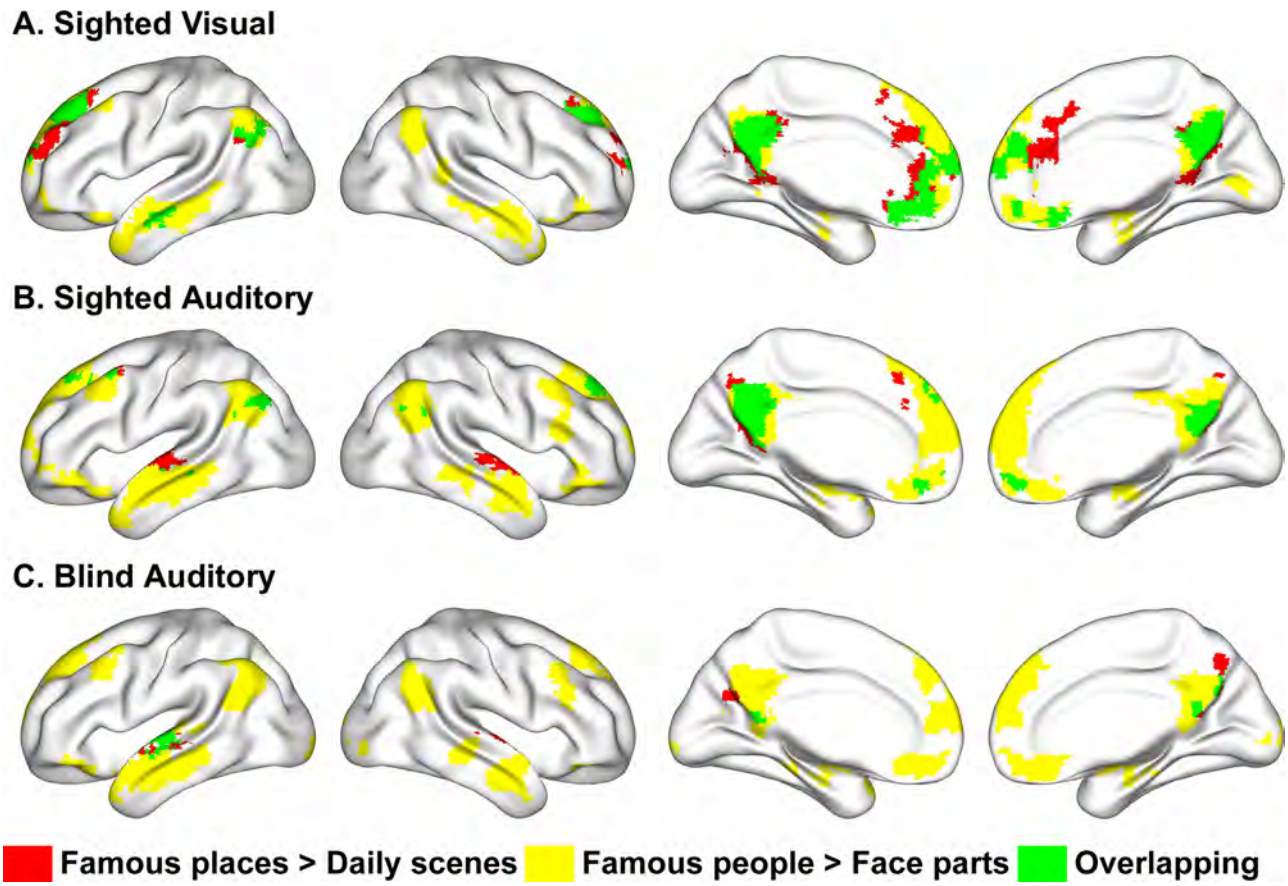

Fig. 2. Maps of unique entity effects in A) sighted visual, B) sighted auditory and C) blind auditory experiments. Red patches indicate brain regions showing significantly stronger activity to famous places compared to daily scenes; yellow patches indicate brain regions showing significantly stronger activity to famous people compared to face parts; green patches indicate overlapping regions of the two contrasts. The significance threshold for each contrast was set to the AlphaSim corrected $p < 0.05$ (single voxel $p < 0.01$, cluster size ≥ 891 mm^3). (For interpretation of the references to color in this figure legend, the reader is referred to the web version of this article.)

person categories, and that these effects were equally strong in the blind and sighted groups. The functional response profile within each ROI is further presented in Fig. 3, with beta values for each category (versus rest) extracted and plotted for all experiments (sighted visual, sighted auditory, blind auditory) for each ROI. Validation analyses based on ROIs defined by the contrast of famous places and daily scenes identified highly similar results (Supplementary Materials).

Table 3
Results of ANOVAs (F values) within ROIs showing unique entity effects for both place and people categories in the sighted visual experiments (green patches in Fig. 1).

	PCC/medPrec	medPFC	Left ATL	Left TPJ	Right SFG
People category: Famous people vs. face parts					
$U/F_{(1,27)}$	111.08***	129.61***	86.54***	75.56***	48.00***
$G/F_{(1,27)}$	3.85	0.76	3.86	0.04	0.63
$U \times G/F_{(1,27)}$	0.54	0.22	0.10	1.24	0.07
Place category: Famous places vs. daily scenes					
$U/F_{(1,27)}$	22.78***	4.24*	7.97*	11.00**	8.87**
$G/F_{(1,27)}$	2.42	2.41	4.19	1.59	1.07
$U \times G/F_{(1,27)}$	0.04	0.43	0.35	1.36	2.39

Notes: U: main effect for uniqueness; G: main effect for group (Sighted vs. Blind); U × G: Interaction effect between uniqueness and group;*: $p < 0.05$;**: $p < 0.01$;***: $p < 0.001$.

3.4. *Unique entity effects across categories and experiments: whole-brain conjunction analyses*

We further investigated the unique entity effects across the whole brain in blind and sighted auditory experiments. Regions showing a significant preference for unique entities in each of the two auditory experiments were defined similarly as in the sighted visual experiment. The resulting regions (Fig. 2(B) and (C), green patches) were then superimposed on the regions found in the sighted visual experiment (Fig. 2(A), green patches) to reveal unique entity specific regions independent of visual input and visual experience. As shown in Fig. 4(A), overlapping regions across both categories and all three experiments (dark red patches) were observed in the bilateral PCC/medPrec. In addition, clusters in bilateral medPFC, bilateral SFG and left TPJ showed significant unique entity effects across categories in the sighted visual and sighted auditory experiments (blue patches).

As the conjunction method is quite conservative (Caria et al., 2012; Nichols et al., 2005), especially in the case of more than 2 contrasts, we lowered the threshold to uncorrected $p < 0.05$ for each contrast in each experiment to observe potential consistency across categories and experiments. By lowering the threshold, regions showing unique entity effect across both categories and all three experiments (dark red patches in Fig. 4(B)) were observed in the bilateral PCC/medPrec, bilateral SFG, left TPJ and in left medPFC. In the left ATL, there was a small overlap (not visible on the surface in Fig. 4(B)) between a cluster showing cross-category unique entity effects across the sighted visual and sighted auditory experiments (blue temporal cluster in Fig. 4(B)) and a cluster showing cross-category unique entity effects across the sighted visual and blind auditory experiments (cyan temporal cluster in Fig. 4(B)). The middle part of the left STG exhibited cross-category unique entity effects in both auditory experiments (orange temporal cluster in Fig. 4(B)). This might reflect the word length difference between unique and common entities (longer word stimuli for unique entities, Appendix) or mismatch of other aspects of low-level word features. We thus focused on the results obtained in both the auditory experiments and the visual experiments, where different types of stimuli were used (words vs. pictures) and the low level effects specific to one type of stimuli could be excluded (conjunction results across experiments in Fig. 4, dark red regions).

Taken together, the whole-brain conjunction analyses are in line with the ROI findings, showing that unique entity effects in the

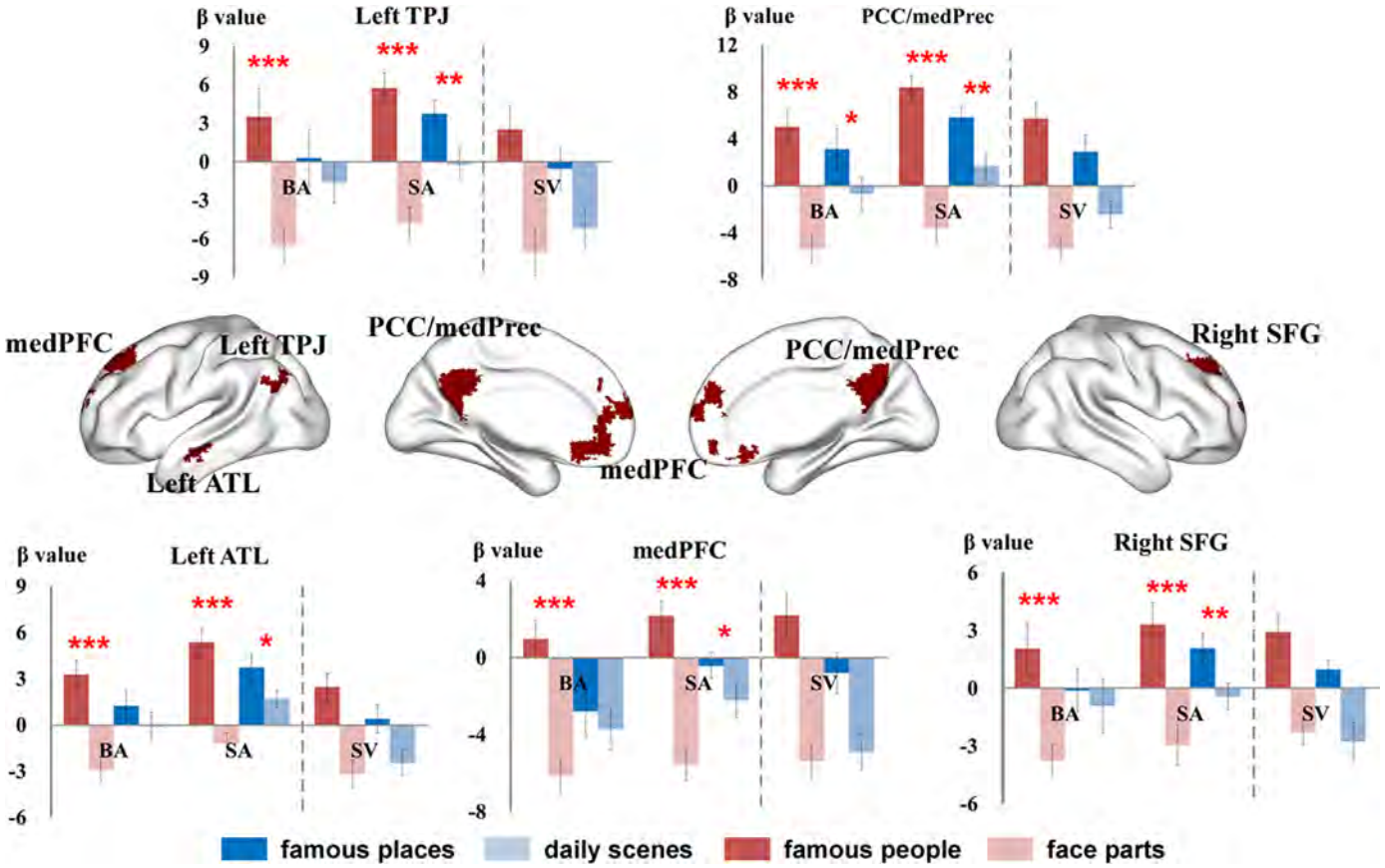

Fig. 3. Activity in the sighted and blind auditory experiments within unique-entity ROIs defined by the sighted visual experiment (green patches in Fig. 2). The y-axis denotes the beta value of brain activation relative to rest. The bars for the sighted visual experiment (on the right side of the dashed line) are presented for comparison with the auditory experiments. BA: blind auditory experiment; SA: sighted auditory experiment; SV: sighted visual experiment. Asterisks denote the significance level of the post-hoc *t*-test of uniqueness effect. ***: $p < 0.001$. **: $p < 0.01$,*: $p < 0.05$. (For interpretation of the references to color in this figure legend, the reader is referred to the web version of this article.)

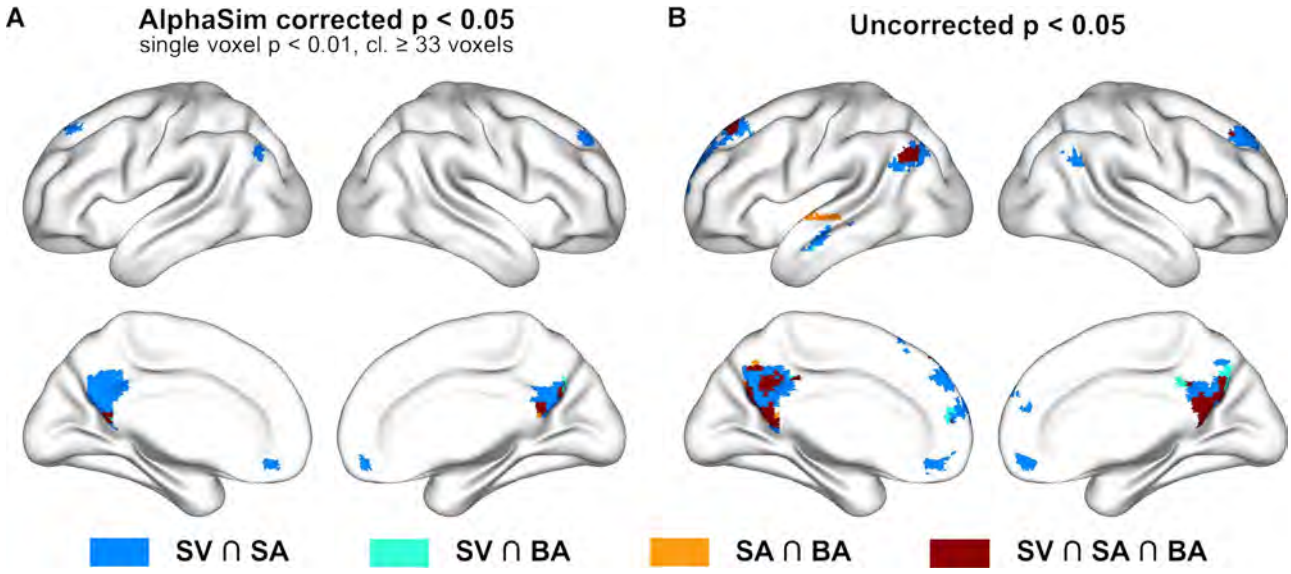

Fig. 4. Conjunction maps of regions showing unique entity effects to both place and people categories for two or three experiments. Note that each experiment result was itself a conjunction of place and people category effects. A) conjunction map of regions showing significant unique entity effects, with each contrast thresholded at AlphaSim corrected $p < 0.05$ (single voxel $p < 0.01$, cluster size ≥ 891 mm^3); B) conjunction map of regions showing significant unique entity effects, with each contrast thresholded at uncorrected $p < 0.05$. In both figures, dark red patches indicate overlapping regions across all three experiments; orange patches indicate overlapping regions across the two auditory experiments; blue patches indicate overlapping regions across sighted visual and sighted auditory experiments; cyan patches indicate overlapping regions across sighted visual and blind auditory experiments. BA: blind auditory experiment; SA: sighted auditory experiment; SV: sighted visual experiment. (For interpretation of the references to color in this figure legend, the reader is referred to the web version of this article.)

bilateral PCC/medPrec, medPFC, left TPJ, right SFG and left ATL were largely independent of visual experience. These results were also confirmed by the validation analyses based exclusively on the contrast between famous places and daily scenes (Supplementary Materials).

3.5. *Regions showing significant uniqueness-by-group interaction effects*

As revealed by whole-brain group-by-uniqueness ANOVAs, a cluster in the right posterior inferior occipital cortex showed a significant group–by-uniqueness interaction effect in both place and people categories (Fig. 5, yellow patch). Interestingly, this region showed a significant unique entity preference in the blind ($t_{(25)}=2.58$, $p < 0.02$, averaged across place and people categories), but showed the opposite pattern in the sighted ($t_{(31)}=-5.25$, $p < 0.0001$). There were also broader regions showing an interaction for the place contrast only, including the right cingulate and supplemental motor area, bilateral temporal and postcentral/precentral regions (Fig. 5, blue patches), with the general trend of showing the generic-entity advantage in the sighted group only (data not shown here for simplicity). The causes for such group differences remain to be further investigated.

Whole-brain ANOVAs also identified brain regions showing significant uniqueness effects and group effects respectively. Detailed results concerning the main effects are reported in the Supplementary Materials. Briefly here, for both categories, bilateral PCC/medPrec, medPFC, left ATL, left TPJ, bilateral SFG and bilateral superior temporal cortex were identified as showing significant main effect of uniqueness, with a preference for famous entities (Supp. Fig. 1), which is highly similar to the results we observed above in Section 3.3 (Fig. 4); the bilateral posterior occipital/temporal cortex showed a significant main effect of group, with significantly stronger responses in the blind auditory experiment (Supp. Fig. 2), which is consistent with previous findings that the visual cortex of blind people shows plastic functional

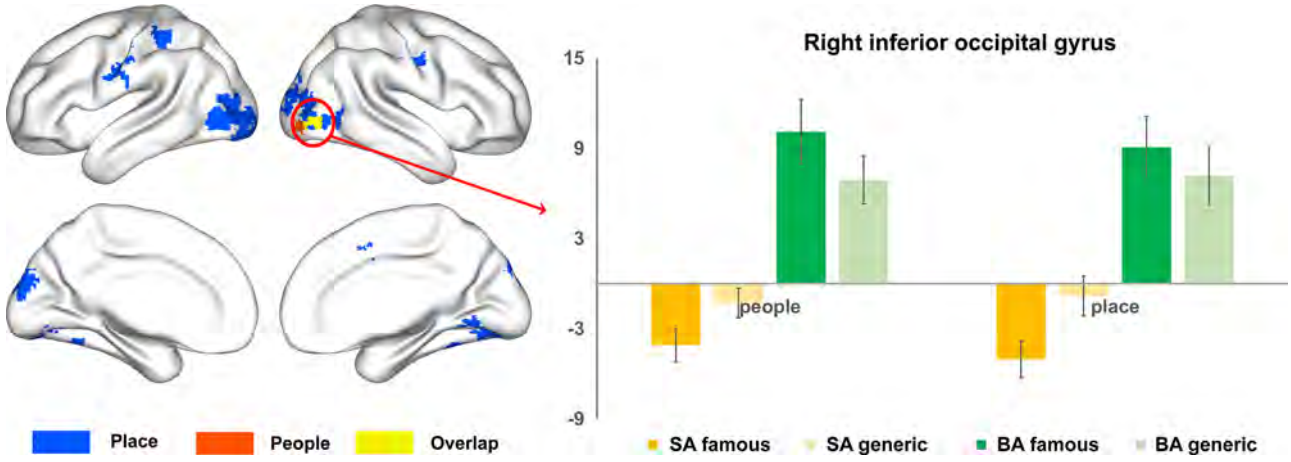

Fig. 5. Regions showing significant uniqueness-by-group interaction effects across place and people categories. Blue patches indicate brain regions showing significant interaction effect for the place category and red patch indicates those for the people category; yellow patch indicates overlapping regions across the two categories. BA: blind auditory experiment; SA: sighted auditory experiment. (For interpretation of the references to color in this figure legend, the reader is referred to the web version of this article.)

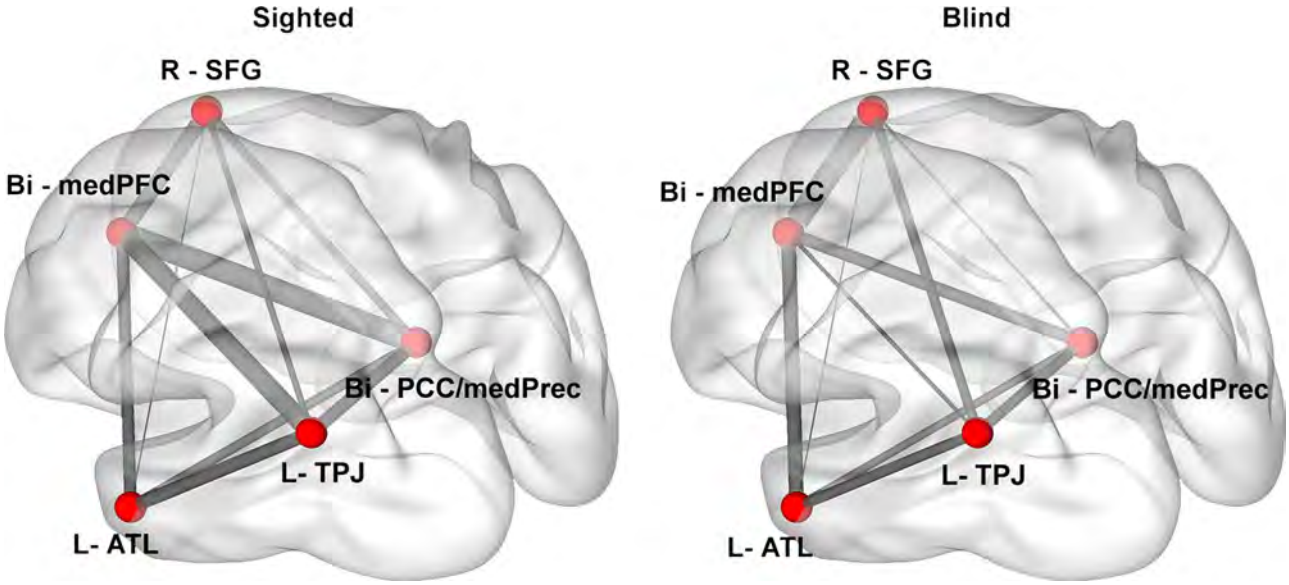

Fig. 6. Similar intrinsic functional brain networks for unique entity processing in the sighted and congenitally blind groups. The width of the edge indicates the connectivity strengths between seed ROIs (range of median *r*: blind: 0.49–0.70; sighted: 0.34 – 0.65). R: right; L: left; Bi: bilateral.

Table 4
Resting-state functional connectivity matrix of the ROIs showing unique entity effects for both place and people categories in the sighted visual experiments. T values are presented, with degrees of freedom shown in the left-most column. RSFCs with control site are indicated by italics.

		PCC/medPrec	medPFC	Left ATL	Left TPJ	Right SFG
	medPFC	7.23***				
Blind	Left ATL	7.95***	10.37***			
$t_{(11)}$	Left TPJ	10.17***	12.80***	10.80***		
	Right SFG	8.48***	12.11***	9.53***	13.55***	
	Left LOTC	*2.95*	*1.00*	*0.81*	*2.35*	*1.85*
		PCC/medPrec	medPFC	Left ATL	Left TPJ	Right SFG
	medPFC	21.84***				
Sighted	Left ATL	13.87***	19.68***			
$t_{(33)}$	Left TPJ	20.44***	23.39***	22.42***		
	Right SFG	12.59***	19.82***	10.42***	14.13***	
	Left LOTC	*1.88*	*0.49*	*0.41*	*2.58*	*0.53*
		PCC/medPrec	medPFC	Left ATL	Left TPJ	Right SFG
	medPFC	−0.99				
Sighted vs. Blind	Left ATL	−0.49	−1.16			
$t_{(44)}$	Left TPJ	−1.57	0.63	−0.24		
	Right SFG	−2.18	−0.73	−1.91	−0.94	
	Left LOTC	*−1.95*	*−0.81*	*−1.12*	*−1.18*	*−1.58*

Notes: *: $p < 0.05$;**: $p < 0.01$;***: $p < 0.001$; Bonferroni corrected.

reorganization to auditory stimuli (Collignon et al., 2011; Noppeney, 2007; Pascual-Leone et al., 2005).

3.6. The intrinsic unique entity network: resting-state functional connectivity analysis

To test for intrinsic or spontaneous functional connectivity between the regions showing unique-entity effects, and to test whether this connectivity pattern is modulated by visual experience, we carried out resting-state functional connectivity (RSFC) analysis in both the blind and sighted groups, using the five ROIs (green patches in Fig. 2) identified by the intersection of place and people unique-entity effects in the sighted visual experiments. In both groups, the five ROIs were significantly connected to each other (Bonferroni corrected, alpha < 0.05, sighted: $t_{(33)} > 10.42$, blind: $t_{(11)} > 7.23$, see Fig. 6 and Table 4). In the between-group comparison, no significant differences ($|t_{s(44)}| < 2.18$) were observed for the RSFC strengths between any ROI pairs (Table 4) after Bonferroni correction, indicating that these brain regions are interconnected with each other to form a network underlying the processing of unique entities in both sighted and congenitally blind individuals.

By contrast, we did not observe any significant connections between the unique entity selective ROIs and a control region in left lateral occipitotemporal cortex (see Section 2.6) in either of the two groups after Bonferroni correction (Table 4, italics), indicating that the tight interconnections between the unique-entity related ROIs we observed was not driven by some general confounding factor but reflect intrinsic synchronization that may be a critical basis for unique entity processing.

4. Discussion

The present study examined the role of visual experience in the representation of unique entities. Contrasting pictures of famous places and people with pictures of their common counterparts revealed activation in a network of brain regions that includes bilateral PCC/medPrec, bilateral medPFC, left ATL, left TPJ and right

SFG. Region of interest analyses and whole-brain conjunction analyses revealed that all these regions also showed a significant unique entity preference when congenitally blind and sighted participants listened to the names of unique entities. Furthermore, resting-state functional connectivity analyses revealed that these regions spontaneously connected tightly with each other but not with functionally distinct control sites in both sighted and blind groups. Together, these results provide evidence for a visually-independent brain network for the processing of unique entities. These findings extend recent research on the functional organization of higher-order cortex of congenitally/early blind individuals, further supporting the hypothesis of a modality-independent, supramodal organization of the human brain, i. e., exhibiting qualitatively similar task-related activation patterns across multiple sensory modalities even if overall activation strengths may differ across modalities or groups (Bedny et al., 2009; Bi et al., 2016; Kitada et al., 2014, 2013; Ricciardi et al., 2013).

An important aspect of the current study was the inclusion of two categories: places and people. In the main analyses, we focused on results that were common to these two categories, following previous work on unique entity processing (Gorno-Tempini and Price, 2001; Grabowski et al., 2001; Ross and Olson, 2012). While we observed several regions that appeared selective for the famous > non-famous contrast involving one of the two categories only (for sighted visual experiment, see Fig. 2), we are cautious in interpreting these results, as the two categories had different control conditions: the famous people category was contrasted with face parts (with slight task differences), whereas the famous places category was contrasted with generic places (this was due to the constraints of the auditory task). While results of one of these contrasts might reflect multiple processes/effects, including differences in low-level visual features (e.g., the lingual and calcarine activation for the famous people vs. face parts contrast), category-selective representations or task differences, activation common to both contrasts is likely to reflect properties that are more strongly associated with unique entities relative to generic items irrespective of category or specific control conditions. Note that this is not to say that different types of unique entities necessarily form one uniform “unique category” or that they entail representations in these regions to the same degree. In fact, several studies have observed brain regions selective to one of these categories, as well as selectivity for specific categories at different sub-sections of ATL, at individual, kind, and common levels (e.g., Fairhall and Caramazza, 2013; Fairhall et al., 2014; Gorno-Tempini and Price, 2001). Our analyses here highlight the finding that independently of whether the representations in the observed sites differ across categories, they are all more relevant for unique items than for generic items. Indeed, the validation analyses using only the contrast between famous places and daily scenes yielded highly similar results to those obtained in the main analyses combining both the people and the place categories.

The regions we found are highly consistent with previous studies investigating the neural substrates underlying unique entity processing (Damasio et al., 1996; Fairhall and Caramazza, 2013; Fairhall et al., 2014; Gesierich et al., 2012; Gorno-Tempini and Price, 2001; Gorno-Tempini et al., 1998; Grabowski et al., 2001; Nakamura et al., 2000; Ross and Olson, 2012; Tranel, 2006). As noted in the Introduction, specific aspects of the unique entity effects observed in the previous literature might be visually driven, induced by attention-modulated visual specification (van Belle et al., 2010) or the interaction between visual attention and episodic memory retrieval (Guerin et al., 2012) of visually presented unique entities, or richer and finer visual imagery of verbally-presented unique items. Importantly, the finding that bilateral PCC/medPrec, medPFC, left ATL, left TPJ and right SFG showed similar unique entity effects in the congenitally blind and sighted groups during auditory processing excludes a purely visual account for these regions' roles in unique entity processing.

If not due to visual processes, what nonvisual properties drive the preference to unique entities in these regions? As mentioned in the Introduction, unique entities are distinguished from their common counterparts on at least the following aspects: unique entities 1) have more specific semantic associations; 2) are often denoted by a proper name; and 3) are often associated with rich and more specific episodic memory. Besides, it has also been proposed that unique entities 4) are more frequently involved in social interaction and thus have higher social significance (Ross and Olson, 2012). These characteristics, which do not necessarily rely on visual experience, might contribute to the unique entity effects in these regions. The first two aspects – semantic specificity and names – might explain specific activations in response to unique entities in the left ATL, as previous literature has characterized this region as a convergence zone that associates stored semantic knowledge with proper names (Belfi and Tranel, 2014; Damasio et al., 2004, 1996; Gorno-Tempini and Price, 2001; Grabowski et al., 2001; Ross and Olson, 2012; Tranel, 2006) or a general semantic hub involved when differentiation of specific-level concepts is required (Patterson et al., 2007; Rogers et al., 2006; Tyler et al., 2004). In particular, by manipulating the information (semantic uniqueness, semantic richness, presence/absence of a proper name) associated with the novel face/place stimuli in a training paradigm, Ross and Olson (2012) found that the activity in left ATL was modulated by both unique semantic information and proper names. Noteworthy, while traditionally ventral ATL regions have been found to be multi-modal and sensitive to semantic specificity (Lambon Ralph, 2014; Visser and Lambon Ralph, 2011; Visser et al., 2010), the left ATL region we found was located more dorsally. The absence of the ventral ATL might be related to insufficient signal coverage in this part (Halai et al., 2014; Visser et al., 2010). Indeed, we computed the temporal signal-to-noise ratio (tSNR) maps (Fan et al., 2013) for each of the three experiments (Supp. Fig. 5), and found that the ventral part of ATLs had relatively low signal quality which could lead to low detection power (Murphy et al., 2007). As suggested by previous findings that the left TPJ might be engaged in lexical retrieval (Gesierich et al., 2012; Gorno-Tempini et al., 2004) or semantic processing (Binder et al., 2009; Gesierich et al., 2012), the first two characteristics might also account for the unique entity effects in the left TPJ.

The unique entity effects in the left TPJ as well as in bilateral PCC/medPrec and medPFC might be related to the last two characteristics of unique entities – episodic retrieval and social interaction – as these regions have been frequently reported to be involved in episodic memory processing and/or social cognition (Bedny et al., 2009; Buckner and Carroll, 2007; Cabeza et al., 2008; Carter and Huettel, 2013; Cavanna and Trimble, 2006; Hassabis and Maguire, 2007; Hassabis et al., 2007; Lepage et al., 2000; Maguire et al., 2001; Sestieri et al., 2011; Svoboda et al., 2006). Interestingly, these properties, especially those related to social cognition, are particularly salient for person items, and thus the preference to person-related knowledge in earlier studies can be similarly accommodated (e.g., Fairhall et al., 2014). It is also possible that unique entities as compared to their common counterparts are more “interesting” and salient and thus more strongly engage attention, which might explain the preference for unique entities in brain regions involved in attention modulation and cognitive control such as the left TPJ and right SFG (Carter and Huettel, 2013; Ptak, 2012). In sum, the unique entity effects we found are not visually dependent and might result from processes such as semantic specification, lexical retrieval, episodic retrieval or social cognitive processes, which are not necessarily visually based. The exact roles these regions play in unique entity processing remain to be investigated further.

In addition to the above regions showing unique entity preferences in both sighted and blind groups, we observed a

significant group-by-uniqueness interaction for both the people and place categories in a cluster of the right posterior inferior occipital cortex. This region showed stronger activation to famous entities in the blind group but not in the sighted group (Section 3.5.). This additional unique-entity preferring region in the blind might be due to plastic changes of occipital cortex caused by the lack of visual input. For instance, blind people's primary visual cortex has been shown to be associated with episodic retrieval (Raz et al., 2005) and language processing (Bedny et al., 2011). These are both possible variables underlying the uniqueness effect.

Interestingly, in addition to similarity in terms of regional activation profiles in bilateral PCC/medPrec, bilateral medPFC, left ATL, left TPJ and right SFG regions across sighted and blind groups, we found significant RSFC between each pair of the above regions in both groups. Furthermore, these regions were tightly connected with each other but not with a functionally distinct object shape related control region. While these results leave open the possibility that unique-entity preferring regions are additionally connected to other brain regions outside of the unique entity network, they provide a plausible network basis for the representation of unique entities that is independent of visual experience.

This interconnected visually-independent brain network underlying unique entity processing largely overlaps with previously described brain networks that have been linked to multiple distinct functions: the theory of mind network (Gallagher and Frith, 2003; Mahy et al., 2014), the semantic network (Binder et al., 2009) and the network for episodic memory processing (Rugg and Vilberg, 2013). In particular, the unique entity network is highly similar to the default-mode network (Biswal et al., 2010; Buckner et al., 2008; Raichle, 2015), which has been shown to be deactivated during explicit tasks compared to rest, with the extent of deactivation being correlated with task difficulty (Buckner et al., 2008; Fox et al., 2005; Gilbert et al., 2012; Harrison et al., 2011; Humphreys et al., 2015). Interestingly, in most cases the unique entity preferring regions exhibited positive activation to unique entities (see Fig. 3) in our study, indicating that the unique effects we obtained could not be merely driven by task difficulty effects. The overlap of these multiple networks points to various possible cognitive processes that might underlie unique entity processing. It is possible that some shared underlying component(s) across different cognitive processes are at stake; it is also possible that the unique entity preferring brain regions are visible across different systems because they play highly integrative roles. Indeed, these interconnected regions were also identified as cortical hubs of the intrinsic human brain network (Buckner et al., 2009). Why and how these regions evolved or developed to link tightly with each other and to be engaged in various cognitive processes including unique entity processing, and the exact roles that these regions play in unique entity processing, warrant further investigation.

In summary, we found a similar set of brain regions underlying the processing of unique entities in congenitally blind and sighted participants across visual and nonvisual tasks. Resting-state functional connectivity showed that in both groups, these regions connected to each other to form a tightly linked intrinsic functional network. Our results suggest that the neural mechanisms for unique entities develops and functions without visual input or visual experience. The correspondence between sighted and congenitally blind participants might be explained by an intrinsic brain network for processing of abstract or linguistically based semantic, social or episodic contents of unique entities.

Funding

This work was supported by National Key Basic Research Program of China (2013CB837300 and 2014CB846103 to Y. B.), NSFC (31500882 to X.W, 31221003 to Y.B., 31271115 to Z. H.,), NCET (12-0055 to Y. B.; 12-0065 to Z. H.), Fok Ying Tong Education Foundation (141020 to Y. B.) and the Fondazione Cassa di Risparmio di Trento e Rovereto (A. C.).

Notes

We thank Dr. Chenxi He for helpful discussions, Drs Xueming Lu and Yujun Ma for help with data analyses and BNU-CNLab members for assistance in data collection.

Conflict of Interest

The authors declare no competing financial interests.

Appendix A. Supplementary material

Supplementary data associated with this article can be found in the online version at http://dx.doi.org/10.1016/j.neuropsychologia.2016.05.007.

Appendix

See Table A1.

Table A1
Complete List of Stimuli (original Chinese stimuli in parentheses).

Famous people	Famous places	Face parts	Daily scenes
Jackie Chen (成龙)	White House (白宫)	Tip of nose (鼻头)	Supermarket (超市)
Teresa Teng (邓丽君)	Beihai Park (北海)	Nose (鼻子)	Castle (城堡)
Deng Xiaoping (邓小平)	Beijing Railway Station (北京站)	Forehead (额头)	Kitchen (厨房)
Ge You (葛优)	Potala Palace (布达拉宫)	Earlobe (耳垂)	Bridge (大桥)
Gong Li (巩俐)	Forbidden City (故宫)	Ear (耳朵)	Edifice (大厦)
Hu Jintao (胡锦涛)	National Center for the Performing Arts (国家大剧院)	Moustache (胡子)	Palace (宫殿)
Li Guyi (李谷一)	Pyramid (金字塔)	Eyelashes (睫毛)	Classroom (教室)
Lu Xun (鲁迅)	Beijing National Stadium (鸟巢)	Cheek (脸颊)	Church (教堂)
Mao Zedong (毛泽东)	Great Hall of the People (人民大会堂)	Eyebrows (眉毛)	Theatre (剧院)
Na Ying (那英)	Beijing National Aquatics Center (水立方)	Tongue (舌头)	Living room (客厅)
Ni Ping (倪萍)	Tian'anmen (天安门)	Pupil (瞳孔)	Pavilion (凉亭)
Song Dandan (宋丹丹)	Temple of Heaven (天坛)	Hair (头发)	Dining Hall (食堂)
Soong Ching-ling (宋庆龄)	Beijing West Railway Station (西客站)	Chin (下巴)	Study (书房)
Song Zuying (宋祖英)	Opera Australia (悉尼歌剧院)	Teeth (牙齿)	Bedroom (卧室)
Wen Jiabao (温家宝)	CCTV Headquarters (央视大楼)	Eyelid (眼睑)	Balcony (阳台)
Yang Lan (杨澜)	Summer Palace (颐和园)	Eye (眼睛)	Hospital (医院)
Yao Ming (姚明)	Old Summer Palace (圆明园)	Lips (嘴唇)	Bathroom (浴室)
Zhou Enlai (周恩来)	Great Wall of China (长城)	Corner of mouth (嘴角)	Corridor (走廊)

References

Anzellotti, S., Caramazza, A., 2014. The neural mechanisms for the recognition of face identity in humans. Front. Psychol. 5, 672.

Bedny, M., Pascual-Leone, A., Dodell-Feder, D., Fedorenko, E., Saxe, R., 2011. Language processing in the occipital cortex of congenitally blind adults. Proc. Natl. Acad. Sci. U. S. A. 108, 4429–4434.

Bedny, M., Pascual-Leone, A., Saxe, R.R., 2009. Growing up blind does not change the neural bases of Theory of Mind. Proc. Natl. Acad. Sci. U.S.A. 106, 11312–11317.

Belfi, A.M., Tranel, D., 2014. Impaired naming of famous musical melodies is associated with left temporal polar damage. Neuropsychology 28, 429–435.

Bi, Y., Wang, X., Caramazza, A., 2016. Object domain and modality in the ventral visual pathway. Trends Cogn. Sci. 20, 282–290.

Binder, J.R., Desai, R.H., 2011. The neurobiology of semantic memory. Trends Cogn. Sci. 15, 527–536.

Binder, J.R., Desai, R.H., Graves, W.W., Conant, L.L., 2009. Where is the semantic system? A critical review and meta-analysis of 120 functional neuroimaging studies. Cereb. Cortex 19, 2767–2796.

Biswal, B.B., Mennes, M., Zuo, X.-N., Gohel, S., Kelly, C., Smith, S.M., Beckmann, C.F., Adelstein, J.S., Buckner, R.L., Colcombe, S., Dogonowski, A.-M., Ernst, M., Fair, D., Hampson, M., Hoptman, M.J., Hyde, J.S., Kiviniemi, V.J., Kötter, R., Li, S.-J., Lin, C.-P., Lowe, M.J., Mackay, C., Madden, D.J., Madsen, K.H.,, Margulies, D.S., Mayberg, H.S., McMahon, K., Monk, C.S., Mostofsky, S.H., Nagel, B.J., Pekar, J.J., Peltier, S.J., Petersen, S.E., Riedl, V., Rombouts, S.A.R.B, Rypma, B., Schlaggar, B.L., Schmidt, S., Seidler, R.D., Siegle, G.J., Sorg, C., Teng, G.-J., Veijola, J., Villringer, A., Walter, M., Wang, L., Weng, X.-C., Whitfield-Gabrieli, S., Williamson, P., Windischberger, C., Zang, Y.-F., Zhang, H.-Y., Castellanos, F.X., Milham, M.P., 2010. Toward discovery science of human brain function. Proc. Natl. Acad. Sci. U. S. A. 107, 4734–4739.

Buckner, R.L., Andrews-Hanna, J.R., Schacter, D.L., 2008. The brain's default network: anatomy, function, and relevance to disease. Ann. N. Y. Acad. Sci. 1124, 1–38.

Buckner, R.L., Carroll, D.C., 2007. Self-projection and the brain. Trends Cogn. Sci. 11, 49–57.

Buckner, R.L., Petersen, S.E., Ojemann, J.G., Miezin, F.M., Squire, L.R., Raichle, M.E., 1995. Functional anatomical studies of explicit and implicit memory retrieval tasks. J. Neurosci. 15, 12–29.

Buckner, R.L., Sepulcre, J., Talukdar, T., Krienen, F.M., Liu, H., Hedden, T., Andrews-Hanna, J.R., Sperling, R.A., Johnson, K.A., 2009. Cortical hubs revealed by intrinsic functional connectivity: mapping, assessment of stability, and relation to Alzheimer's disease. J. Neurosci. 29, 1860–1873.

Cabeza, R., Ciaramelli, E., Olson, I.R., Moscovitch, M., 2008. The parietal cortex and episodic memory: an attentional account. Nat. Rev. Neurosci. 9, 613–625.

Caria, A., Falco, S., de, Venuti, P., Lee, S., Esposito, G., Rigo, P., Birbaumer, N., Bornstein, M.H., 2012. Species-specific response to human infant faces in the premotor cortex. Neuroimage 60, 884–893.

Carter, R.M., Huettel, S. a, 2013. A nexus model of the temporal-parietal junction. Trends Cogn. Sci. 17, 328–336.

Cavanna, A.E., Trimble, M.R., 2006. The precuneus: a review of its functional anatomy and behavioural correlates. Brain 129, 564–583.

Chao-Gan, Y., Yu-Feng, Z., 2010. DPARSF: A MATLAB Toolbox for "Pipeline" Data Analysis of Resting-State fMRI. Front. Syst. Neurosci. 4, 13.

Collignon, O., Vandewalle, G., Voss, P., Albouy, G., Charbonneau, G., Lassonde, M., Lepore, F., 2011. Functional specialization for auditory-spatial processing in the occipital cortex of congenitally blind humans. Proc. Natl. Acad. Sci. U. S. A. 108, 4435–4440.

Damasio, H., Grabowski, T.J., Tranel, D., Hichwa, R.D., Damasio, A.R., 1996. A neural basis for lexical retrieval. Nature 380, 499–505.

Damasio, H., Tranel, D., Grabowski, T., Adolphs, R., Damasio, A., 2004. Neural systems behind word and concept retrieval. Cognition 92, 179–229.

Fairhall, S.L., Anzellotti, S., Ubaldi, S., Caramazza, A., 2014. Person- and place-selective neural substrates for entity-specific semantic access. Cereb. Cortex 24, 1687–1696.

Fairhall, S.L., Caramazza, A., 2013. Category-selective neural substrates for person- and place-related concepts. Cortex 49, 2748–2757.

Fan, L., Wang, J., Zhang, Y., Han, W., Yu, C., Jiang, T., 2013. Connectivity-based parcellation of the human temporal pole using diffusion tensor imaging. Cereb. Cortex, 96.

Fletcher, P.C., Frith, C.D., Baker, S.C., Shallice, T., Frackowiak, R.S., Dolan, R.J., 1995. The mind's eye–precuneus activation in memory-related imagery. Neuroimage 2, 195–200.

Fletcher, P.C., Shallice, T., Frith, C.D., Frackowiak, R.S., Dolan, R.J., 1996. Brain activity during memory retrieval. The influence of imagery and semantic cueing. Brain 119 (5), 1587–1596.

Fox, M.D., Snyder, A.Z., Vincent, J.L., Corbetta, M., Van Essen, D.C., Raichle, M.E., 2005. The human brain is intrinsically organized into dynamic, anticorrelated functional networks. Proc. Natl. Acad. Sci. U. S. A. 102, 9673–9678.

Freiwald, W.A., Tsao, D.Y., 2010. Functional compartmentalization and viewpoint generalization within the macaque face-processing system. Science 330, 845–851. http://dx.doi.org/10.1126/science.1194908.

Gallagher, H.L., Frith, C.D., 2003. Functional imaging of "theory of mind". Trends Cogn. Sci. 7 (2), 77–83.

Gesierich, B., Jovicich, J., Riello, M., Adriani, M., Monti, A., Brentari, V., Robinson, S.D., Wilson, S.M., Fairhall, S.L., Gorno-Tempini, M.L., 2012. Distinct neural substrates for semantic knowledge and naming in the temporoparietal network. Cereb. Cortex 22, 2217–2226.

Ghazanfar, A., Schroeder, C., 2006. Is neocortex essentially multisensory? Trends Cogn. Sci. 10, 278–285.

Gilbert, S.J., Bird, G., Frith, C.D., Burgess, P.W., 2012. Does "task difficulty" explain "task-induced deactivation?". Front. Psychol. 3, 125.

Gorno-Tempini, M.L., Dronkers, N.F., Rankin, K.P., Ogar, J.M., Phengrasamy, L., Rosen, H.J., Johnson, J.K., Weiner, M.W., Miller, B.L., 2004. Cognition and anatomy in three variants of primary progressive aphasia. Ann. Neurol. 55, 335–346.

Gorno-Tempini, M.L., Price, C.J., 2001. Identification of famous faces and buildings: a functional neuroimaging study of semantically unique items. Brain 124, 2087–2097.

Gorno-Tempini, M.L., Price, C.J., Josephs, O., Vandenberghe, R., Cappa, S.F., Kapur, N., Frackowiak, R.S., Tempini, M.L., 1998. The neural systems sustaining face and proper-name processing. Brain 121 (11), 2103–2118.

Grabowski, T.J., Damasio, H., Tranel, D., Ponto, L.L., Hichwa, R.D., Damasio, a R., 2001. A role for left temporal pole in the retrieval of words for unique entities. Hum. Brain Mapp. 13, 199–212.

Gross, C.G., 1994. How inferior temporal cortex became a visual area. Cereb. Cortex 4, 455–469.

Gross, C.G., Bender, D.B., Rocha-Miranda, C.E., 1969. Visual receptive fields of neurons in inferotemporal cortex of the monkey. Science 166, 1303–1306.

Guerin, S.A., Robbins, C.A., Gilmore, A.W., Schacter, D.L., 2012. Interactions between visual attention and episodic retrieval: dissociable contributions of parietal regions during gist-based false recognition. Neuron 75, 1122–1134.

Halai, A.D., Welbourne, S.R., Embleton, K., Parkes, L.M., 2014. A comparison of dual gradient-echo and spin-echo fMRI of the inferior temporal lobe. Hum. Brain Mapp. 35, 4118–4128.

Halsband, U., Krause, B.J., Schmidt, D., Herzog, H., Tellmann, L., Müller-Gärtner, H. W., 1998. Encoding and retrieval in declarative learning: a positron emission tomography study. Behav. Brain Res. 97, 69–78.

Harrison, B.J., Pujol, J., Contreras-Rodríguez, O., Soriano-Mas, C., López-Solà, M., Deus, J., Ortiz, H., Blanco-Hinojo, L., Alonso, P., Hernández-Ribas, R., Cardoner, N., Menchón, J.M., 2011. Task-Induced deactivation from rest extends beyond the default mode brain network. PLoS. One, 6.

Hassabis, D., Kumaran, D., Maguire, E.A., 2007. Using imagination to understand the neural basis of episodic memory. J. Neurosci. 27, 14365–14374.

Hassabis, D., Maguire, E. a, 2007. Deconstructing episodic memory with construction. Trends Cogn. Sci. 11, 299–306.

He, C., Peelen, M.V., Han, Z., Lin, N., Caramazza, A., Bi, Y., 2013. Selectivity for large nonmanipulable objects in scene-selective visual cortex does not require visual experience. Neuroimage 79, 1–9.

Humphreys, G.F., Hoffman, P., Visser, M., Binney, R.J., Lambon Ralph, M.A., 2015. Establishing task- and modality-dependent dissociations between the semantic and default mode networks. Proc. Natl. Acad. Sci. 112, 201422760..

Kitada, R., Okamoto, Y., Sasaki, A.T., Kochiyama, T., Miyahara, M., Lederman, S.J., Sadato, N., 2013. Early visual experience and the recognition of basic facial expressions: involvement of the middle temporal and inferior frontal gyri during haptic identification by the early blind. Front. Hum. Neurosci. 7, 7.

Kitada, R., Yoshihara, K., Sasaki, A.T., Hashiguchi, M., Kochiyama, T., Sadato, N., 2014. The brain network underlying the recognition of hand gestures in the blind: the supramodal role of the extrastriate body area. J. Neurosci. 34, 10096–10108.

Krause, B.J., Schmidt, D., Mottaghy, F.M., Taylor, J., Halsband, U., Herzog, H., Tellmann, L., Müller-Gärtner, H.W., 1999. Episodic retrieval activates the precuneus irrespective of the imagery content of word pair associates. A PET study. Brain 122. 2, 255–263.

Kravitz, D.J., Saleem, K.S., Baker, C.I., Ungerleider, L.G., Mishkin, M., 2013. The ventral visual pathway: an expanded neural framework for the processing of object quality. Trends Cogn. Sci. 17 (1), 26–49.

Kriegeskorte, N., Formisano, E., Sorger, B., Goebel, R., 2007. Individual faces elicit distinct response patterns in human anterior temporal cortex. Proc. Natl. Acad. Sci. U. S. A. 104, 20600–20605.

Lambon Ralph, M.A., 2014. Neurocognitive insights on conceptual knowledge and its breakdown. Philos. Trans. R. Soc. Lond. B. Biol. Sci. 369, 20120392.

Lepage, M., Ghaffar, O., Nyberg, L., Tulving, E., 2000. Prefrontal cortex and episodic memory retrieval mode. Proc. Natl. Acad. Sci. U. S. A. 97, 506–511.

Maguire, E.A., Vargha-Khadem, F., Mishkin, M., 2001. The effects of bilateral hippocampal damage on fMRI regional activations and interactions during memory retrieval. Brain 124, 1156–1170.

Mahon, B.Z., Anzellotti, S., Schwarzbach, J., Zampini, M., Caramazza, A., 2009. Category-specific organization in the human brain does not require visual experience. Neuron 63, 397–405.

Mahy, C.E.V., Moses, L.J., Pfeifer, J.H., 2014. How and where: theory-of-mind in the brain. Dev. Cogn. Neurosci. 9, 68–81.

Murphy, K., Bodurka, J., Bandettini, P.A., 2007. How long to scan? The relationship between fMRI temporal signal to noise ratio and necessary scan duration. Neuroimage 34, 565–574.

Nakamura, K., Kawashima, R., Sato, N., Nakamura, A., Sugiura, M., Kato, T., Hatano, K., Ito, K., Fukuda, H., Schormann, T., Zilles, K., 2000. Functional delineation of the human occipito-temporal areas related to face and scene processing. A PET study. Brain 123, 1903–1912.

Nichols, T., Brett, M., Andersson, J., Wager, T., Poline, J.-B., 2005. Valid conjunction inference with the minimum statistic. Neuroimage 25, 653–660.

Noppeney, U., 2007. The effects of visual deprivation on functional and structural organization of the human brain. Neurosci. Biobehav. Rev. 31, 1169–1180.

Pascual-Leone, A., Amedi, A., Fregni, F., Merabet, L.B., 2005. The plastic human brain

cortex. Annu. Rev. Neurosci. 28, 377–401.
Patterson, K., Nestor, P.J., Rogers, T.T., 2007. Where do you know what you know? The representation of semantic knowledge in the human brain. Nat. Rev. Neurosci. 8, 976–987.
Peelen, M.V., Bracci, S., Lu, X., He, C., Caramazza, A., Bi, Y., 2013. Tool selectivity in left occipitotemporal. Cortex Dev. Vis., 1225–1234.
Peelen, M.V., He, C., Han, Z., Caramazza, A., Bi, Y., 2014. Nonvisual and visual object shape representations in occipitotemporal cortex: evidence from congenitally blind and sighted adults. J. Neurosci. 34, 163–170.
Ptak, R., 2012. The frontoparietal attention network of the human. Brain : Action, Sali., a Prior. Map Environ. 18 (5), 502–515.
Raichle, M.E., 2015. The Brain's Default Mode Network. Annu. Rev. Neurosci. 38, 433–447.
Raz, N., Amedi, A., Zohary, E., 2005. V1 activation in congenitally blind humans is associated with episodic retrieval. Cereb. Cortex 15, 1459–1468.
Ricciardi, E., Bonino, D., Pellegrini, S., Pietrini, P., 2013. Mind the blind brain to understand the sighted one! Is there a supramodal cortical functional architecture? Neurosci. Biobehav. Rev. 41, 64–77.
Rogers, T.T., Hocking, J., Noppeney, U., Mechelli, A., Gorno-Tempini, M.L., Patterson, K., Price, C.J., 2006. Anterior temporal cortex and semantic memory: reconciling findings from neuropsychology and functional imaging. Cogn. Affect. Behav. Neurosci. 6, 201–213.
Ross, L. a, Olson, I.R., 2012. What's unique about unique entities? An fMRI investigation of the semantics of famous faces and landmarks. Cereb. Cortex 22, 2005–2015.
Rugg, M.D., Vilberg, K.L., 2013. Brain networks underlying episodic memory retrieval. Curr. Opin. Neurobiol. 23 (2), 255–260.
Schneider, W., Eschman, A., Zuccolotto, A., 2002. E-Prime reference guide. Psychol. Softw. Tools 3, 1.
Sestieri, C., Corbetta, M., Romani, G.L., Shulman, G.L., 2011. Episodic memory retrieval, parietal cortex, and the default mode network: functional and topographic analyses. J. Neurosci. 31, 4407–4420.
Song, X.-W., Dong, Z.-Y., Long, X.-Y., Li, S.-F., Zuo, X.-N., Zhu, C.-Z., He, Y., Yan, C.-G., Zang, Y.-F., 2011. REST: a toolkit for resting-state functional magnetic resonance imaging data processing. PLoS. One. 6 (9), e25031.
Svoboda, E., McKinnon, M.C., Levine, B., 2006. The functional neuroanatomy of autobiographical memory: a meta-analysis. Neuropsychologia 44, 2189–2208.
Tranel, D., 2006. Impaired naming of unique landmarks is associated with left temporal polar damage. Neuropsychology 20, 1–10.
Tyler, L.K., Stamatakis, E.A., Bright, P., Acres, K., Abdallah, S., Rodd, J.M., Moss, H.E., 2004. Processing objects at different levels of specificity. J. Cogn. Neurosci. 16, 351–362.
Tzourio-Mazoyer, N., Landeau, B., Papathanassiou, D., Crivello, F., Etard, O., Delcroix, N., Mazoyer, B., Joliot, M., 2002. Automated anatomical labeling of activations in SPM using a macroscopic anatomical parcellation of the MNI MRI single-subject brain. Neuroimage 15, 273–289.
van Belle, G., Ramon, M., Lefèvre, P., Rossion, B., 2010. Fixation patterns during recognition of personally familiar and unfamiliar faces. Front. Psychol. 1, 20.
Visser, M., Jefferies, E., Lambon Ralph, M. a, 2010. Semantic processing in the anterior temporal lobes: a meta-analysis of the functional neuroimaging literature. J. Cogn. Neurosci. 22, 1083–1094.
Visser, M., Lambon Ralph, M.A., 2011. Differential contributions of bilateral ventral anterior temporal lobe and left anterior superior temporal gyrus to semantic processes. J. Cogn. Neurosci. 23, 3121–3131.
Wang, X., Peelen, M.V., Han, Z., He, C., Caramazza, A., Bi, Y., 2015. How visual is the visual cortex? comparing connectional and functional fingerprints between congenitally blind and sighted individuals. J. Neurosci. 35, 12545–12559.
Wei, T., Liang, X., He, Y., Zang, Y., Han, Z., Caramazza, A., Bi, Y., 2012. Predicting conceptual processing capacity from spontaneous neuronal activity of the left middle temporal gyrus. J. Neurosci. 32, 481–489.
Xia, M., Wang, J., He, Y., 2013. BrainNet Viewer: a network visualization tool for human brain connectomics. PLoS. One 8, e68910.